Article

The Rate Capability Performance of High-Areal-Capacity Water-Based NMC811 Electrodes: The Role of Binders and Current Collectors

Yuri Surace *, Marcus Jahn and Damian M. Cupid

Battery Technologies, Center for Transport Technologies, AIT Austrian Institute of Technology GmbH, Giefinggasse 4, 1210 Vienna, Austria
* Correspondence: yuri.surace@ait.ac.at

Abstract: The aqueous processing of cathode materials for lithium-ion batteries (LIBs) has both environmental and cost benefits. However, high-loading, water-based electrodes from the layered oxides (e.g., NMC) typically exhibit worse electrochemical performance than NMP-based electrodes. In this work, primary, binary, and ternary binder mixtures of aqueous binders such as CMC, PAA, PEO, SBR, and Na alginate, in combination with bare and C-coated Al current collectors, were explored, aiming to improve the rate capability performance of NMC811 electrodes with high areal capacity (≥ 4 mAh cm^{-2}) and low binder content (3 wt.%). Electrodes with a ternary binder composition (CMC:PAA:SBR) have the best performance with bare Al current collectors, attaining a specific capacity of 150 mAh g^{-1} at 1C. Using carbon-coated Al current collectors results in improved performance for both water- and NMP-based electrodes. This is further accentuated for Na-Alg and CMC:PAA binder compositions. These electrodes show specific capacities of 170 and 80 mAh g^{-1} at 1C and 2C, respectively. Although the specific capacities at 1C are comparable to those for NMP-PVDF electrodes, they are approximately 50% higher at the 2C rate. This study aims to contribute to the development of sustainably processed NMC electrodes for high energy density LIBs using water as solvent.

Keywords: NMC811; aqueous processing; high-loading electrodes; water-based electrodes; aqueous binders; carbon-coated aluminum current collector; rate capability

1. Introduction

Research efforts in the last three decades have resulted in a steady increase in the performance (energy, safety, and stability) of Li-ion batteries (LIBs), leading to their integration into electric vehicles (EVs). Car manufacturers have increased the number of EVs in their fleet and successfully introduced them into the mass market, with 200 million EVs expected to be sold by 2030 [1]. In such a fast-growing, competitive market, the cost and the environmental impact of LIB production play a major role. A crucial step in battery manufacturing is the processing of anode and cathode active materials to produce electrode coatings [2,3]. While commercial anode electrodes (i.e., based on graphite or silicon–graphite) are already produced using water as a solvent combined with water-based binders, cathode electrodes (i.e., based on LiNi$_x$Mn$_x$Co$_x$O$_2$ (NMC), LiNi$_{0.5}$Mn$_{1.5}$O$_4$ (LNMO), etc.) are still largely processed using organic solvents, specifically N-methyl-2-pyrrolidone (NMP) with poly(vinylidene difluoride) (PVDF) as the binder. The NMP-PVDF combination has many disadvantages. Firstly, the PVDF binder is considerably more expensive than water-soluble binders and is not easy to dispose of at the end of the battery life [4].

Indeed, PVDF has raised environmental concerns primarily due to its high fluorine content and the fact that PVDF is not readily biodegradable. During manufacturing, use, and disposal, fluoropolymers such as PVDF may release perfluorinated compounds (PFCs) into the environment, which are known for their bioaccumulation and toxic properties [5].

Also, fluoropolymers have recently been included in a restriction proposal within the European Union. Secondly, NMP is costly and toxic [4], and its higher boiling point than water results in larger energy consumption during the electrode drying step [6]. Furthermore, NMP is a volatile organic compound (VOC) and needs solvent recovery at a commercial scale, making the electrode manufacturing process very expensive [7].

On the other hand, water-soluble binders such as Na-carboxymethylcellulose (Na-CMC), styrene-butadiene rubber (SBR), polyacrylic acid (PAA), and Na alginate are not only cheaper but also easier to recycle [4]. Additionally, the use of water as a solvent removes the need for solvent recovery [6]. It is then clear that switching to water-based processing for cathode materials will also decrease the cost and improve the sustainability of LIB production. However, aqueous cathode processing has many challenges. Firstly, the cathode active material is unstable in water due to the leaching of Li^+ ions and Li^+/H^+ ion exchange. This causes changes on the surface of the active material (i.e., the formation of LiOH surface impurities and Li- and oxygen-depleted surface layers, as well as the phase transitions of near-surface layers [8]) and gives rise to solutions with very high pH values (~12) [9,10]. In turn, the high pH leads to the corrosion of the current collector and bubble evolution during the coating process [11]. Consequently, the electrodes usually show cracks and pinholes [11]. Secondly, the high surface tension of water produces a high capillary pressure during drying [12], which once again leads to crack formation and poor electrode flexibility. These issues are even more enhanced for thick coatings, which are needed to achieve high energy density cells. Therefore, the electrochemical performance of water-based cathode electrodes is generally poorer than those processed using NMP [10,12].

Various approaches have been investigated to overcome these issues. Leaching can be compensated with novel cell architectures such as the reserve LIBs [13]. With respect to the slurry, while the pH can be easily controlled and lowered below the Al corrosion threshold through the addition of acids [14–16], coping with the high surface tension of water, due to being an intrinsic property, requires more effort in finding the right inactive slurry components (i.e., type of conductive carbon [11,17], binder [18–24], co-solvents such as alcohols [12,18], etc.) and slurry formulation (i.e., ratio and amount of the slurry components [18,20,22,25]), which results in a homogeneous, flexible and defect-free coating with good electrochemical properties.

Although the binder is an inactive component in slurry and electrode formulations, it performs a very important role as it ensures the interconnection and electronic contact between the active material and conductive carbon particles, provides adhesion to the current collector, and promotes electrode flexibility [26,27]. While PVDF is the main option for NMP-based slurries, especially at an industrial scale, there are several binder choices for aqueous cathode slurries. Therefore, binder selection is crucial for determining the mechanical properties and electrochemical performance. This becomes even more important for high areal loading/capacity electrodes ($\geq$20 mg cm^{-2}, $\geq$4 mAh cm^{-2}), which are required for practical applications. However, most of the reports investigating water-based binders usually include low areal loading/capacity electrodes (5–10 mg cm^{-2} 1–2 mAh cm^{-2}) [15,21,22,24,28,29], which are relevant only for lab-scale experiments.

Another inactive electrode component that plays a crucial role in influencing the performance of aqueous slurries is the Al current collector. Indeed, it has been shown that the utilization of carbon-coated Al current collectors reduces corrosion [30,31] and indirectly improves the electrode quality by decreasing the number of electrode defects during and after processing. Furthermore, the chemical interaction between the carbon coating layer and water-based binders such as CMC [32] resulted in improved electrochemical performance.

To the best of our knowledge, a systematic study on the influence of the binder, including binder–current collector interactions, on the rate capability of high-areal-capacity NMC electrodes is lacking. Therefore, in this work, NMC811 electrodes with commercially relevant areal capacity (~4 mAh/cm^2), high active material content (>90 wt.%), and low binder amount (3 wt.%) were produced through aqueous processing. Our goal was to understand the influence of different parameters such as the type of binder, the binder

mixture, and the binder–current collector combination on the electrochemical performance, with a particular focus on improving the rate capability. By varying the above-listed parameters, we were able to determine the best binder mixture–current collector combination to achieve comparable and in some specific cases better performance than the PVDF-based electrodes of similar areal capacity.

2. Materials and Methods

2.1. Materials

The following materials were used for the electrode preparation: NMC811 (T81RX, d_{90} = 20.7, S_{BET} = 0.35 m^2 g^{-1}, Targray, Kirkland, Canada); "C-NERGY" SuperC45 conductive carbon (average particle size = 37 nm, S_{BET} = 45 m^2 g^{-1}, Imerys Graphite and Carbon, Bironico, Switzerland); sodium carboxymethyl cellulose (CMC, M.W. 250 k, degree of substitution 0.9, Sigma-Aldrich, St. Louis, MO, United States); polyacrylic acid (PAA, M.W. 450 k, Sigma-Aldrich, St. Louis, MO, USA); phosphoric acid (H_3PO_4, Sigma-Aldrich, St. Louis, MO, USA); polyethylene oxide (PEO, M.W. 600 k, Acros Organics, Geel, Belgium); styrene-butadiene rubber (SBR, TRD104A, ENEOS Materials, Leuven, Belgium); sodium alginate binder (Sigma-Aldrich, St. Louis, MO, USA); and PVDF 5120 (Solef® PVDF, Solvay SA, Brussels, Belgium). All materials were used as received unless stated otherwise.

2.2. Electrode Preparation

A summary of the electrodes investigated, along with the nomenclature used in this paper, is presented in Table 1. Electrode slurries were prepared in batches of 5 g. The weight ratios of active and inactive components, i.e., NMC811:SuperC45:binder, were kept constant at 92:5:3 for all electrodes.

Table 1. An overview of the investigated electrodes.

Electrode Name	Binder Type	Binder Amount (wt.%)	Current Collector Type
3CMC/Al	Na-CMC	3	Al
3PAA/Al	PAA	3	Al
3PEO/Al	PEO	3	Al
1CMC:2PAA/Al	Na-CMC:PAA	3 (1:2)	Al
1CMC:2SBR/Al	Na-CMC:SBR	3 (1:2)	Al
1CMC:1PAA:1SBR/Al	Na-CMC:PAA:SBR	3 (1:1:1)	Al
3PVDF/Al	PVDF	3	Al
3CMC/C-Al	Na-CMC	3	C-coated Al
3PAA/C-Al	PAA	3	C-coated Al
3Alg/C-Al	Na-Alginate	3	C-coated Al
1CMC:2PAA/C-Al	Na-CMC:PAA	3 (1:2)	C-coated Al
1CMC:2SBR/C-Al	Na-CMC:SBR	3 (1:2)	C-coated Al
1CMC:1PAA:1SBR/C-Al	Na-CMC:PAA:SBR	3 (1:1:1)	C-coated Al
3PVDF/C-Al	PVDF	3	C-coated Al

In a standard preparation, the binder was initially dissolved in the solvent. A water–isopropanol mixture of 80:20 wt.% [12] was used for all the binders except for CMC:SBR, in which only water was used, and except for PVDF, in which NMP was used. After this dissolution process, the SC45 conductive additive was added and blended with the binder solution for 2 min. Then, H_3PO_4 was added and stirred for 1 min. In the last step, NMC811 was added, and the slurry was homogenized for 2 min. A total of 0.16 mmol of H_3PO_4 per 1 g of NMC811 was added prior to the addition of NMC to control the pH value throughout

the mixing process. The amount of solvent was adjusted to achieve a solid content of 50% (45% for Na alginate). The stirring was performed with a turbo-stirrer (Ultra-Turrax T18, IKA, Staufen, Germany) at 16,000 RPM. After 1 h of degassing on a roller–mixer, the pH was measured (SevenCompact S210, Mettler-Toledo, Greifensee, Switzerland) just before coating the slurry onto the current collector. The pH values were always below the threshold of 9.0 to prevent the corrosion of the Al current collector [33]. The slurries were then cast onto either an aluminum current collector (Al-CC) (15 μm, MTI corporation, Richmond, CA, USA) or a carbon-coated aluminum current collector (C-coated Al-CC) (20 μm + 1 μm carbon, Cambridge Energy Solutions, Cambridge, UK) using the doctor-blade technique. The cast electrode sheets were dried under vacuum at 80 °C overnight. The electrodes had an average areal loading of 20.5 ± 1.0 mg/cm^2 and were calendered to a density of 3.1 ± 0.1 g/cm^3.

Circular electrodes of 15 mm diameter were punched out and re-dried overnight using a Büchi® glass oven at 120 °C under vacuum to remove any remaining traces of water.

2.3. Electrochemical Characterization

The electrodes were assembled in an argon-filled glove box (<0.1 ppm H$_2$O and <0.1 ppm O$_2$) into coin-type cells with metallic lithium ($\geq$99.9%, thickness 0.75 mm, Alfa Aesar, Ward Hill, MA, USA) as a counter electrode and a glass fiber separator. The electrolyte used in this study was 1 M LiPF$_6$ comprising ethylene carbonate (EC)–ethyl methyl carbonate (EMC) (3:7 vol.%) + 2 wt.% vinylidene carbonate (VC) (Solvionic, France). The electrochemical measurements were carried out with a battery cycler (Maccor series 4000, Tulsa, OK, USA) at 25 °C. The rate capability tests were performed by changing the current rate every five cycles according to the following constant current–constant potential (CCCP) cycling procedure: C/10 (charge)-C/10 (discharge), C/5-C/5, C/4-C/4, C/4-C/3, C/4-C/2, C/4-1C, C/4-2C, C/4-4C, and C/10-C/10, for a total of 45 cycles. A constant potential (CP) step with a limit set to 10% of the current rate of the specific cycle was applied at the end of the charge. The current rate was calculated based on a theoretical specific capacity of 200 mAh g^{-1} for NMC811. The potential cut-off limits were set to 3.0 V and 4.3 V vs. Li$^+$/Li. The specific capacity is presented per mass of electroactive material. To ensure reproducibility, for each given set of conditions, the data of at least two cells were taken into account, including the calculation of the standard deviation. For clarity of presentation, the average value with the standard deviation (shown as a shaded area) of only the discharge capacity is shown in the performance graphs.

3. Results and Discussion

3.1. Influence of the Binder Type

In the first step of our work, high-areal-capacity NMC electrodes were prepared with different water-based binders in a primary binder composition, i.e., using only one type of binder and maintaining the amount of binder constant to 3 wt.%.

The rate capability performance values of NMC811 electrodes with 3 wt.% PAA, 3 wt.% CMC, and 3 wt.% PEO aqueous binders coated on Al-CC are shown in Figure 1. Figure 1a includes the specific discharge capacities of the electrodes as a function of cycle number, whereas Figure 1b shows the relative capacities of the electrodes, which is defined as the percentage ratio of the discharge capacity at cycle *n* to the discharge capacity of the third cycle. Electrodes prepared with 3 wt.% PVDF in the NMP solvent are also shown for reference. The respective first-cycle coulombic efficiency and potential profiles are shown in Figure S1 and Figure S2, respectively.

The first-cycle coulombic efficiency for the tested electrodes varied between 87% and 89% (Figure S1, Table S1), with 3PAA/Al and 3CMC/Al showing the lowest (87.5%) and highest (89.5%) values, respectively, among the primary binder compositions coated on Al-CC. Surprisingly, 3CMC/Al electrodes had a higher first-cycle coulombic efficiency than 3PVDF/Al. At a low discharge rate of C/10, the specific capacities of the electrodes was in the order 3PVDF/Al (202 mAh g^{-1}) > 3CMC/Al (196 mAh g^{-1}) > 3PEO/Al (192 mAh g^{-1})

> 3PAA/Al (186 mAh g^{-1}). The same trend was maintained for the C/5 and C/4 rates, with a slight decrease in capacity to 94–96% of the initial value. Notably, 3PEO/Al electrodes showed a marked decrease in capacity already at C/3, which became even more pronounced at C/2, when the capacity dropped to only 70 mAh g^{-1}. The reason for this capacity fading can be related to the poor adhesion [34] and low ionic conductivity [35] of PEO, making this binder unsuitable for high-rate applications.
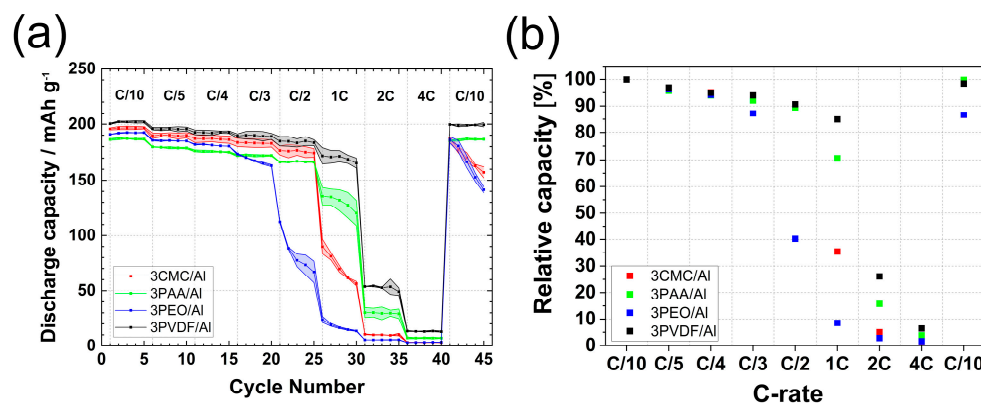

Figure 1. (**a**) Discharge capacity vs. cycle number; (**b**) relative capacity vs. C rate of 3CMC/Al, 3PAA/Al, 3PEO/Al, and 3PVDF/Al electrodes.

The specific capacities of the 3CMC/Al, 3PAA/Al, and 3PVDF/Al electrodes were in the range of 180–190 mAh g^{-1} and 170–180 mAh g^{-1} at C/3 and C/2, respectively; therefore, they decreased to around 92–94% and 89–91% of the capacity at C/10, respectively. Increasing the current rate to 1C revealed a clear difference between the electrodes based on PVDF compared to those based on aqueous binders. Notably, 3PVDF/Al electrodes yielded around 170 mAh g^{-1} at 1C, whereas 3PAA/Al and 3CMC/Al electrodes yielded only around 120–130 mAh g^{-1} and 70–80 mAh g^{-1}, respectively. Specifically, the 3CMC/Al electrodes rapidly lost capacity at every single cycle, similar to 3PEO/Al at 0.5C, indicating that electrode degradation might be occurring at these high rates. At 2C, even electrodes with the PVDF binder showed a considerable decrease in capacity to around 50 mAh g^{-1}, which is attributed to the slower Li$^+$ diffusion in high-mass loading electrodes [36]. The 3PAA/Al electrodes yielded 30 mAh g^{-1} at 2C, while 3PEO/Al and 3CMC/Al electrodes showed negligible capacity at this rate. The recovery cycles at C/10 after the rate capability test revealed that only 3PVDF/Al and 3PAA/Al returned to their initial capacities, while 3PEO/Al and 3CMC/Al showed rapid capacity fading. This behavior results from the high rates the electrodes experienced in the previous cycles (break out point: 0.5 C for 3PEO/Al and 1 C for 3CMC/Al) and might be related to either the loss of adhesion to the current collector or the loss of contact between active material particles and the conductive network due to binder degradation.

3.2. Influence of the Binder Mixture

While electrode formulations based on the NMP solvent only use a PVDF binder, water-based cathode slurry formulations typically, but not necessarily, include at least two binders. One is CMC, which acts as a dispersant, binder, and thickening agent to control the viscosity of the slurry, and the second or even third binder is usually chosen between different families such as polyacrylates (PAA), aromatic polymers (SBR), and polysaccharides (alginate, guar gum, etc.) [4,18,37,38]. Therefore, in the second approach, high-areal-capacity electrodes were prepared using binary and ternary binder compositions by combining CMC with either SBR or PAA in a 1:2 ratio, as well as combining these three binders together in a 1:1:1 ratio. The 1:2 ratio was chosen in accordance with previous studies on optimizing electrochemical performance [20], whereas the 1:1:1 ratio was chosen to guarantee the same amount of binder in a ternary composition. The study of different binder ratios is beyond the scope of this paper.

The electrochemical results of the tested electrodes are shown in Figure 2, and the potential profiles are presented in Figure S2. For all binder mixtures, the first-cycle coulombic efficiency of the electrodes was very similar to those for electrodes fabricated using primary binder compositions, i.e., it oscillated between 87% and 89%, with 1CMC:1PAA:1SBR/Al showing the highest CE of 89.3%. At C/10, the 1CMC:1PAA:1SBR/Al electrodes exhibited the same specific capacity as the 3PVDF–Al electrodes, while the 1CMC:2SBR/Al and 1CMC:2PAA/Al electrodes had slightly lower capacities at the same rate. The measured specific capacities on discharge followed the order 3PVDF/Al (202 mAh g^{-1}) > 1CMC:1PAA:1SBR/Al (199 mAh g^{-1}) > 1CMC:2SBR/Al (194 mAh g^{-1}) > 1CMC:2PAA/Al (188 mAh g^{-1}). Between C/5 and C/2, the discharge and relative capacity values of the electrodes prepared with ternary binder compositions were comparable to those obtained for 3PVDF/Al, reaching 180 mAh g^{-1} at C/2, which was 90.5% of the initial capacity. This indicates that, in terms of performance, water-based 1CMC:1PAA:1SBR/Al electrodes can compete against PVDF electrodes up to C/2 rates.
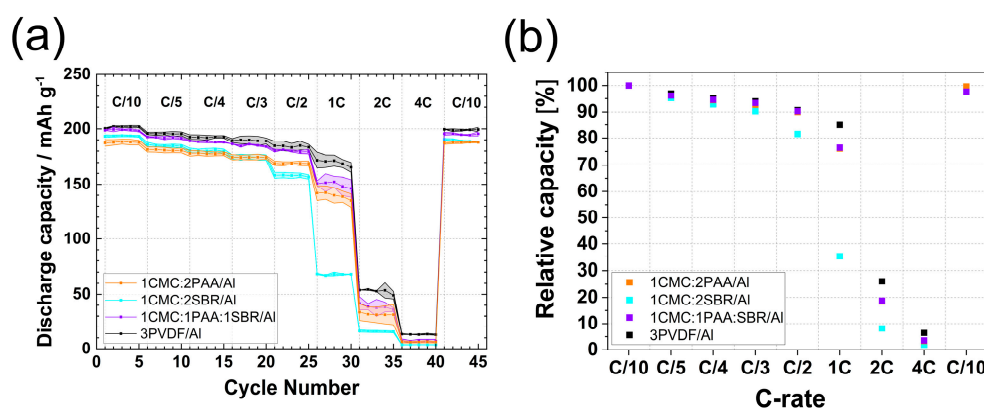

Figure 2. (**a**) Discharge capacity vs. cycle number; (**b**) relative capacity vs. C rate of 1CMC:2PAA/Al, 1CMC:2SBR/Al, 1CMC:1PAA:1SBR/Al, and 3PVDF/Al electrodes.

The capacities of the 1CMC:2SBR/Al and 1CMC:2PAA/Al electrodes almost overlapped from C/5 to C/3, while at C/2, 1CMC:2PAA/Al performed better, with a capacity of 169 mAh g^{-1} instead of 158 mAh g^{-1} for 1CMC:2SBR/Al. At 1C, the 1CMC:2SBR/Al electrodes performed the worst, yielding a capacity of only 70 mAh g^{-1}, while 1CMC:2PAA/Al and 1CMC:1PAA:1SBR/Al electrodes yielded around 140–150 mAh g^{-1}. The relative capacity of 3PVDF/Al was about 9% higher at this rate in comparison to 1CMC:2PAA/Al or 1CMC:1PAA:1SBR/Al, i.e., 85% for 3PVDF/Al vs. 76% for 1CMC:2PAA/Al and 1CMC:1PAA:1SBR/Al.

By further increasing the current rate, the capacity dropped below 50 mAh g^{-1} for all water-based electrodes, and it was slightly above 50 mAh g^{-1} for 3PVDF/Al. The recovery cycles at C/10 after the high rate test showed that all electrodes returned to about 98–99% of their initial capacity.

Summarizing the results of aqueous binders with standard Al-CC, at current rates from C/10 to C/2, 3CMC/Al and 1CMC:1PAA:1SBR/Al electrodes showed comparable rate performance, with capacities only 3–5 mAh g^{-1} lower than PVDF electrodes. However, at higher rates, specifically at 1C, the capacity followed the order 1CMC:1PAA:1SBR/Al > 1CMC:2PAA/Al > 3PAA/Al, with the ternary binder composition offering the highest capacity, also during recovery cycles after the 4C rate.

The best performance of the electrodes with the 1CMC:1PAA:1SBR binder, as well as the good performance of 1CMC:2PAA, can be explained by the interplay of the two following factors: (1) the combination of binders' elastic properties and (2) binder/binder and active material/binder interactions. Regarding the former, the combination of binders typically leads to enhanced elastic properties due to the blending of the individual elastic characteristics of each binder. The combination CMC:SBR, well known for anode electrodes, offers a mix of high Young's modulus from CMC (20–30 MPa) and high elongation at break

from SBR (10–15%) [39,40]. The addition of PAA to the CMC:SBR combination for Ni-rich cathodes is, however, one of the novelties of our paper. Regarding the latter, it is known from the literature that PAA can crosslink with CMC to strengthen the connection between the two binders and improve electrochemical performance. Also, it is known that PAA can crosslink and/or interact by hydrogen bonds to the -OH groups formed on the surface of active material particles to buffer the volume expansion [41]. These interactions have already been demonstrated for Si/Si-Gr anode electrodes. During the aqueous processing of cathode materials, -OH groups are formed on the NMC surface, which is in contact with water. Therefore, hydroxyl groups are expected to interact with aqueous binders such as PAA, CMC, or alginate binders. In this regard, the combination 1CMC:1PAA:1SBR resulted in the best electrochemical performance among the water-based binder combinations on Al-CC. It is noteworthy to mention that, due to the low concentration (i.e., 3 wt.%), the binders were not visible using SEM analysis. Therefore, no conclusions could be drawn on the binders' distribution or on their influence on the electrode microstructure.

3.3. Influence of Binder Type–Current Collector Interaction

Current collectors are indispensable components of LIBs, which connect the active materials to the external circuits. Therefore, they influence the capacity, rate capability, and long-term stability of lithium-ion batteries [42]. Specifically, carbon-coated Al current collectors are known to result in lower contact resistance and improve adhesion. In the case of water-based slurries, such current collectors are more resistant to corrosion [31]. Electrodes with 3 wt.% CMC and 3 wt.% PAA were studied in comparison to the electrodes coated on bare Al-CC. Electrodes coated with the PVDF binder also served as a reference. Due to the poor performance of electrodes with the PEO binder, we decided to disregard this electrode composition for further studies. Instead, we prepared electrodes with Na alginate, a polysaccharide binder known to perform well with both anode [43,44] and cathode materials [15,19,45]. It is worth mentioning that electrodes with 3 wt.% Na alginate coated onto bare Al-CC could not be tested because of the very poor adhesion to the current collector. The rate capability performance of the electrodes with primary binder compositions on carbon-coated Al current collectors is shown in Figure 3, and the potential profiles are presented in Figure S3. The first-cycle CE was 90.5% for 3CMC/C-Al and 91% for 3PAA/C-Al and 3PVDF/C-Al. These values were higher than those for the electrodes prepared with the same binder composition but coated on bare Al-CC. Since the CE is directly correlated to the parasitic reactions occurring within the cell, an increase in CE can be related to a decrease in the parasitic reaction between the electrolyte and the current collector, especially at high voltages, due to carbon coating as well as an improvement in corrosion resistance [46].
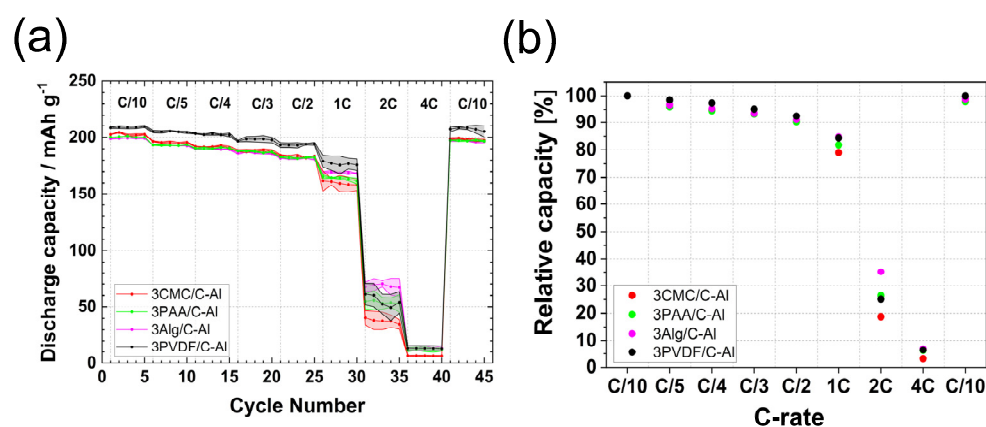

Figure 3. (**a**) Discharge capacity vs. cycle number; (**b**) relative capacity vs. C rate of 3CMC/C-Al, 3PAA/C-Al, 3Na-Alg/C-Al, and 3PVDF/C-Al electrodes.

The 3Alg/C-Al coating configuration instead showed a first-cycle CE of 89%.

At C/10, 3PVDF/C-Al electrodes had a capacity of 209 mAh g^{-1}, about 10 mAh g^{-1} higher than PVDF electrodes coated on bare Al-CC as well as 10 mAh g^{-1} higher than all water-based electrodes with primary binder compositions that were coated on C-coated Al-CC.

Notably, 3CMC/C-Al and 3PAA/C-Al also showed higher initial capacity than 3CMC/Al and 3PAA/Al at C/10; this is due to the lower interfacial resistance with C-Al-CC [32].

Water-based electrodes showed the same capacity between C/5 and C/2, with a decrease in capacity of 2–3% for each rate increase, leading to capacities between 182 and 184 mAh g^{-1} at C/2, which was ~91.5% of the initial capacity. Once the current rate was increased to 1C, the 3Alg/C-Al electrodes were the best-performing water-based electrodes, showing a capacity of 169 mAh g^{-1}. When compared to the relative capacities of the 3PVDF/C-Al electrodes, which yielded a capacity of 176 mAh g^{-1}, the relative capacity of the 3Alg/C-Al electrodes was found to be the same as 3PVDF/C-Al electrodes, i.e., 84%. In addition, 3CMC/C-Al and 3PAA/C-Al electrodes, with a capacity of around 160–165 mAh g^{-1}, showed a considerable improvement in performance in comparison to the 3CMC/Al and 3PAA/Al coating configurations, highlighting once again the important contribution of the C-coated current collector in water-based slurries. Surprisingly, at 2C, the 3Alg/C-Al electrodes performed better than the 3PVDF/C-Al electrodes, yielding around 35% (70 mAh g^{-1}) of the initial capacity.

All water- and NMP-based electrodes returned to their initial capacities during the recovery cycle at C/10. Furthermore, the capacity fading phenomenon observed for 3CMC/Al did not occur for 3CMC/C-Al, probably due to the much better adhesion of the electrode material to the current collector when a carbon coating was used. Generally, by comparing Figures 1 and 3, we can conclude that a clear improvement in specific capacity occurred at all rates for all binder compositions, an indication that the C-coated current collector had an overall positive effect on the performance.

3.4. Influence of Binder Mixture–Current Collector Interaction

Electrodes with binary and ternary binder compositions coated on C-coated Al-CC were also tested and compared with PVDF electrodes on C-coated Al-CC. The first-cycle CE was 88.7% for 1CMC:2SBR/C-Al, 90.0% for 1CMC:2PAA/C-Al, and 89.5% for 1CMC:1PAA:1SBR/C-Al (Figure S1). While the C-coated Al-CC did not improve the first-cycle CE of 1CMC:2SBR/C-Al and 1CMC:1PAA:1SBR/C-Al in comparison to bare Al-CC, a considerable improvement in CE was observed for 1CMC:2PAA/C-Al, i.e., ~2.5%.

The rate capability performance is shown in Figure 4, and the potential profiles are presented in Figure S3. Similar to the electrodes with primary binder compositions, the initial specific capacity at C/10 was around 200 mAh g^{-1} for all binary and ternary binder composition electrodes. Specifically, 1CMC:2PAA/C-Al and 1CMC:2SBR/C-Al showed higher initial capacities than the 1CMC:2PAA/Al and 1CMC:2SBR/Al electrodes with bare Al-CC, while the 1CMC:1PAA:1SBR/C-Al and 1CMC:1PAA:1SBR/Al coating configurations showed the same capacity. Therefore, the influence of the use of carbon-coated Al current collectors on capacity was higher for binary binder combinations than for ternary combinations at low current rates.

The 1CMC:2PAA/C-Al and 1CMC:1PAA:1SBR/C-Al electrodes showed the same performance from C/5 to C/2, while 1CMC:2SBR/C-Al yielded a lower capacity at C/3 and C/2. At C/2, the capacities of 1CMC:2PAA/C-Al and 1CMC:1PAA:1SBR/C-Al were around 183 mAh g^{-1}, which was 92% of the initial capacity, while the capacity of 1CMC:2SBR/C-Al was 170 mAh g^{-1}, 86% of the initial one.

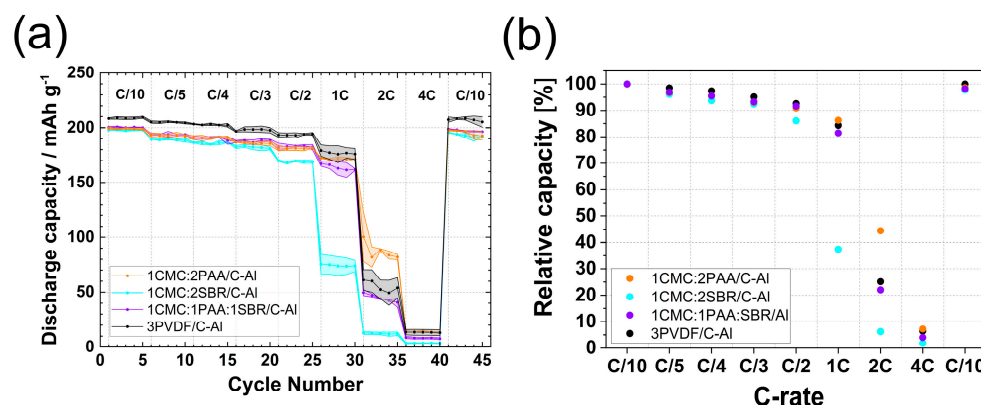**Figure 4.** (**a**) Discharge capacity vs. cycle number; (**b**) relative capacity vs. C rate of 1CMC:2PAA/C-Al, 1CMC:2SBR/C-Al, 1CMC:1PAA:1SBR/C-Al, and 3PVDF/C-Al electrodes.

When the rate was increased to 1C, the best-performing water-based electrodes were 1CMC:2PAA/C-Al. These electrodes had a capacity of 172 mAh g^{-1}, which was 86% of the C/10 capacity. A relative capacity value of 84% was instead attained for the 3PVDF/C-Al electrodes. The capacity of 1CMC:1PAA:1SBR/C-Al and 1CMC:2SBR/C-Al at 1C was 162 mAh g^{-1} and 73 mAh g^{-1}, respectively. Interestingly, with bare Al-CC, the ternary binder compositions resulted in higher capacities, whereas with the C-coated Al-CC, the electrodes with a binary composition containing only CMC and PAA binders performed better. Also, the current collector did not seem to have any influence on the performance of the 1CMC:2SBR binary composition above C/10 rates since the electrodes coated on both current collectors showed very similar performance. Once the rate was increased to 2C, 1CMC:2PAA/C-Al electrodes yielded the highest capacity of 88 mAh g^{-1}, about 30 mAh g^{-1} higher than PVDF electrodes, with a relative capacity of 44%.

All electrodes returned to 98–99% of the initial capacity during the final five recovery cycles at C/10. The use of C-coated Al-CC improved the performance of not only NMC electrodes with primary binder compositions but also those with binary and ternary binder compositions.

The rate capability tests of the electrodes revealed that the C-coated Al current collector affected battery performance differently when using different binder combinations. Furthermore, beyond the factors previously discussed regarding electrodes on bare Al-CC, a new factor comes into play: the interaction between C-coated Al-CC and aqueous binders. This factor is believed to be the key to explaining some performance differences.

Considering the electrodes with primary binder compositions, the main difference in performance was observed at 1C or 2C, i.e., only at high rates. The difference between 3Alg, 3PAA, and 3CMC can be related to the different functional groups of the binders and their ability to crosslink with the current collector. The specific capacities at 1C and 2C were in the order 3Alg > 3PAA > 3CMC; PAA and alginate have carboxylic groups directly connected to the backbone of the polymer. Therefore, the binder backbone in Alg and PAA is closer to the CC than for CMC, ensuring a stronger adhesion between the binder and CC. In addition, alginates, which have different spatial orientations (D-L), are expected to be more efficiently bound to the C-coated Al-CC in comparison to PAA, resulting in even better performance.

Considering instead the electrodes with secondary and ternary binder compositions, a difference in performance was also observed in these cases, mainly at higher rates, except for 1CMC:2SBR, which showed poor performance at high rates with both Al and C-Al-CC. This is probably related to the use of the SBR binder. The better performance of 1CMC:2PAA in comparison to 1CMC:1PAA:1SBR can be related to the higher amount of PAA in the electrode formulation, which may lead to an enhanced crosslink between CMC and PAA and between binders and C-Al-CC.

4. Conclusions

In this work, we investigated the rate capability of high areal capacity, water-based NMC811 electrodes with primary, binary, and ternary binder compositions on bare and C-coated Al-CC. It was found that the inactive electrode components strongly influenced the performance. Using a bare Al-CC, NMC811 electrodes with primary binder composition showed relatively poor rate capability. However, when CMC was combined with PAA, significantly better performance was achieved. Further improvement in rate capability was attained with a ternary binder composition of PAA:CMC:SBR. These electrodes showed the same capacity values as PVDF electrodes from C/10 to C/2, achieving around 150 mAh g^{-1} at the 1C rate.

When switching to a C-coated Al-CC, an overall improvement in first-cycle coulombic efficiency, absolute capacity, and rate capability was observed for water-based electrodes as well as for NMP-based electrodes. Electrodes with the primary binder composition were able to achieve 160–170 mAh g^{-1} at 1 C. Specifically, electrodes with 3 wt.% Na alginate were the best-performing electrodes with the primary binder composition, maintaining 85% of the relative capacity at 1C, similar to the PVDF electrodes. Values of 35% at 2C were attained, which were about 10% better than the PVDF electrodes at a higher rate. The use of C-coated Al CC also prevented capacity fading after faster rates for electrodes with the 3 wt.% CMC binder. Electrodes with binary (CMC:PAA) and ternary (CMC:PAA:SBR) binder compositions showed a relative capacity comparable to the PVDF electrodes between C/5 and C/2 current rates. These electrodes were also able to achieve around 160–170 mAh g^{-1} at 1C, similar to the discharge capacities of the electrodes with the primary binder composition. Moreover, electrodes based on CMC:PAA binders showed a relative capacity of 86% at 1C and 44% at 2C, the highest among the binary and ternary binder compositions and 20% higher than the PVDF electrodes at the faster rate.

References

1. Xu, C.; Dai, Q.; Gaines, L.; Hu, M.; Tukker, A.; Steubing, B. Future material demand for automotive lithium-based batteries. *Commun. Mater.* **2020**, *1*, 99. [CrossRef]
2. Hawley, W.B.; Li, J. Electrode manufacturing for lithium-ion batteries—Analysis of current and next generation processing. *J. Energy Storage* **2019**, *25*, 100862. [CrossRef]
3. Gonçalves, R.; Lanceros-Méndez, S.; Costa, C. Electrode fabrication process and its influence in lithium-ion battery performance: State of the art and future trends. *Electrochem. Commun.* **2022**, *135*, 107210. [CrossRef]
4. Bresser, D.; Buchholz, D.; Moretti, A.; Varzi, A.; Passerini, S. Alternative binders for sustainable electrochemical energy storage—The transition to aqueous electrode processing and bio-derived polymers. *Energy Environ. Sci.* **2018**, *11*, 3096–3127. [CrossRef]

5. Lohmann, R.; Cousins, I.T.; DeWitt, J.C.; Glüge, J.; Goldenman, G.; Herzke, D.; Lindstrom, A.B.; Miller, M.F.; Ng, C.A.; Patton, S.; et al. Are Fluoropolymers Really of Low Concern for Human and Environmental Health and Separate from Other PFAS? *Environ. Sci. Technol.* **2020**, *54*, 12820–12828. [CrossRef] [PubMed]

6. Wood, D.L.; Quass, J.D.; Li, J.; Ahmed, S.; Ventola, D.; Daniel, C. Technical and economic analysis of solvent-based lithium-ion electrode drying with water and NMP. *Dry. Technol.* **2018**, *36*, 234–244. [CrossRef]

7. Wood, D.L., III; Li, J.; Daniel, C. Prospects for reducing the processing cost of lithium ion batteries. *J. Power Sources* **2015**, *275*, 234–242. [CrossRef]

8. Pritzl, D.; Teufl, T.; Freiberg, A.T.S.; Strehle, B.; Sicklinger, J.; Sommer, H.; Hartmann, P.; Gasteiger, H.A. Editors' Choice—Washing of Nickel-Rich Cathode Materials for Lithium-Ion Batteries: Towards a Mechanistic Understanding. *J. Electrochem. Soc.* **2019**, *166*, A4056–A4066. [CrossRef]

9. Hofmann, M.; Kapuschinski, M.; Guntow, U.; Giffin, G.A. Implications of Aqueous Processing for High Energy Density Cathode Materials: Part I. Ni-Rich Layered Oxides. *J. Electrochem. Soc.* **2020**, *167*, 140512. [CrossRef]

10. Wood, M.; Li, J.; Ruther, R.E.; Du, Z.; Self, E.C.; Meyer, H.M., III; Daniel, C.; Belharouak, I.; Wood, D.L., III. Chemical stability and long-term cell performance of low-cobalt, Ni-Rich cathodes prepared by aqueous processing for high-energy Li-Ion batteries. *Energy Stor. Mater.* **2019**, *24*, 188–197. [CrossRef]

11. Sahore, R.; Wood, D.L.; Kukay, A.; Grady, K.M.; Li, J.; Belharouak, I. Towards Understanding of Cracking during Drying of Thick Aqueous-Processed $LiNi_{0.8}Mn_{0.1}Co_{0.1}O_2$ Cathodes. *ACS Sustain. Chem. Eng.* **2020**, *8*, 3162–3169. [CrossRef]

12. Du, Z.; Rollag, K.M.; Li, J.; An, S.J.; Wood, M.; Sheng, Y.; Mukherjee, P.P.; Daniel, C.; Wood, D.L., III. Enabling aqueous processing for crack-free thick electrodes. *J. Power Sources* **2017**, *354*, 200–206. [CrossRef]

13. Parekh, M.H.; Palanisamy, M.; Pol, V.G. Reserve lithium-ion batteries: Deciphering in situ lithiation of lithium-ion free vanadium pentoxide cathode with graphitic anode. *Carbon* **2023**, *203*, 561–570. [CrossRef]

14. Loeffler, N.; Kim, G.-T.; Mueller, F.; Diemant, T.; Kim, J.-K.; Behm, R.J.; Passerini, S. In Situ Coating of Li[Ni0.33Mn0.33Co0.33]O2 Particles to Enable Aqueous Electrode Processing. *ChemSusChem* **2016**, *9*, 1112–1117. [CrossRef] [PubMed]

15. Kazzazi, A.; Bresser, D.; Birrozzi, A.; von Zamory, J.; Hekmatfar, M.; Passerini, S. Comparative Analysis of Aqueous Binders for High-Energy Li-Rich NMC as a Lithium-Ion Cathode and the Impact of Adding Phosphoric Acid. *ACS Appl. Mater. Interfaces* **2018**, *10*, 17214–17222. [CrossRef] [PubMed]

16. Neidhart, L.; Fröhlich, K.; Winter, F.; Jahn, M. Implementing Binder Gradients in Thick Water-Based NMC811 Cathodes via Multi-Layer Coating. *Batteries* **2023**, *9*, 171. [CrossRef]

17. Du, Z.; Li, J.; Wood, M.; Mao, C.; Daniel, C.; Wood, D. Three-dimensional conductive network formed by carbon nanotubes in aqueous processed NMC electrode. *Electrochim. Acta* **2018**, *270*, 54–61. [CrossRef]

18. Ibing, L.; Gallasch, T.; Schneider, P.; Niehoff, P.; Hintennach, A.; Winter, M.; Schappacher, F.M. Towards water based ultra-thick Li ion battery electrodes—A binder approach. *J. Power Sources* **2019**, *423*, 183–191. [CrossRef]

19. Xu, J.; Chou, S.L.; Gu, Q.-F.; Liu, H.K.; Dou, S.X. The effect of different binders on electrochemical properties of LiNi1/3Mn1/3Co1/3O2 cathode material in lithium ion batteries. *J. Power Sources* **2013**, *225*, 172–178. [CrossRef]

20. Li, C.-C.; Wang, Y.-W. Importance of binder compositions to the dispersion and electrochemical properties of water-based $LiCoO_2$ cathodes. *J. Power Sources* **2013**, *227*, 204–210. [CrossRef]

21. Carvalho, D.V.; Loeffler, N.; Hekmatfar, M.; Moretti, A.; Kim, G.-T.; Passerini, S. Evaluation of guar gum-based biopolymers as binders for lithium-ion batteries electrodes. *Electrochim. Acta* **2018**, *265*, 89–97. [CrossRef]

22. Loeffler, N.; Kopel, T.; Kim, G.-T.; Passerini, S. Polyurethane Binder for Aqueous Processing of Li-Ion Battery Electrodes. *J. Electrochem. Soc.* **2015**, *162*, A2692–A2698. [CrossRef]

23. Sahore, R.; Wood, M.; Kukay, A.; Du, Z.; Livingston, K.M.; Wood, D.L.; Li, J. Performance of Different Water-Based Binder Formulations for Ni-Rich Cathodes Evaluated in $LiNi_{0.8}Mn_{0.1}Co_{0.1}O_2$//Graphite Pouch Cells. *J. Electrochem. Soc.* **2022**, *169*, 40567. [CrossRef]

24. Reissig, F.; Puls, S.; Placke, T.; Winter, M.; Schmuch, R.; Gomez-Martin, A. Investigation of Lithium Polyacrylate Binders for Aqueous Processing of Ni-Rich Lithium Layered Oxide Cathodes for Lithium-Ion Batteries. *ChemSusChem* **2022**, *15*, e202200401. [CrossRef] [PubMed]

25. Çetinel, F.A.; Bauer, W. Processing of water-based $LiNi_{1/3}Mn_{1/3}Co_{1/3}O_2$ Pastes for Manufacturing Lithium Ion Battery Cathodes. *Bull. Mater. Sci. Indian Acad. Sci.* **2014**, *37*, 1685–1690. [CrossRef]

26. Lingappan, N.; Kong, L.; Pecht, M. The significance of aqueous binders in lithium-ion batteries. *Renew. Sustain. Energy Rev.* **2021**, *147*, 111227. [CrossRef]

27. Zou, F.; Manthiram, A. A Review of the Design of Advanced Binders for High-Performance Batteries. *Adv. Energy Mater.* **2020**, *10*, 2002508. [CrossRef]

28. Kuenzel, M.; Choi, H.; Wu, F.; Kazzazi, A.; Axmann, P.; Wohlfahrt-Mehrens, M.; Bresser, D.; Passerini, S. Co-Crosslinked Water-Soluble Biopolymers as a Binder for High-Voltage $LiNi_{0.5}Mn_{1.5}O_4$ | Graphite Lithium-Ion Full Cells. *ChemSusChem* **2020**, *13*, 2650–2660. [CrossRef] [PubMed]

29. Loeffler, N.; von Zamory, J.; Laszczynski, N.; Doberdo, I.; Kim, G.-T.; Passerini, S. Performance of LiNi1/3Mn1/3Co1/3O2/graphite batteries based on aqueous binder. *J. Power Sources* **2014**, *248*, 915–922. [CrossRef]

30. Zhu, P.; Gastol, D.; Marshall, J.; Sommerville, R.; Goodship, V.; Kendrick, E. A review of current collectors for lithium-ion batteries. *J. Power Sources* **2021**, *485*, 229321. [CrossRef]

31. Doberdò, I.; Löffler, N.; Laszczynski, N.; Cericola, D.; Penazzi, N.; Bodoardo, S.; Kim, G.-T.; Passerini, S. Enabling aqueous binders for lithium battery cathodes—Carbon coating of aluminum current collector. *J. Power Sources* **2014**, *248*, 1000–1006. [CrossRef]

32. Kuenzel, M.; Bresser, D.; Kim, G.-T.; Axmann, P.; Wohlfahrt-Mehrens, M.; Passerini, S. Unveiling and Amplifying the Benefits of Carbon-Coated Aluminum Current Collectors for Sustainable $LiNi_{0.5}Mn_{1.5}O_4$ Cathodes. *ACS Appl. Energy Mater.* **2020**, *3*, 218–230. [CrossRef]

33. Gabryelczyk, A.; Ivanov, S.; Bund, A.; Lota, G. Corrosion of aluminium current collector in lithium-ion batteries: A review. *J. Energy Storage* **2021**, *43*, 103226. [CrossRef]

34. Qin, T.; Yang, H.; Li, Q.; Yu, X.; Li, H. Design of functional binders for high-specific-energy lithium-ion batteries: From molecular structure to electrode properties. *Ind. Chem. Mater.* **2024**. [CrossRef]

35. Liu, P.; Counihan, M.J.; Zhu, Y.; Connell, J.G.; Sharon, D.; Patel, S.N.; Redfern, P.C.; Zapol, P.; Markovic, N.M.; Nealey, P.F.; et al. Increasing Ionic Conductivity of Poly(ethylene oxide) by Reaction with Metallic Li. *Adv. Energy Sustain. Res.* **2022**, *3*, 2100142. [CrossRef]

36. Gao, H.; Wu, Q.; Hu, Y.; Zheng, J.P.; Amine, K.; Chen, Z. Revealing the Rate-Limiting Li-Ion Diffusion Pathway in Ultrathick Electrodes for Li-Ion Batteries. *J. Phys. Chem. Lett.* **2018**, *9*, 5100–5104. [CrossRef] [PubMed]

37. Hawley, W.B.; Meyer, H.M.; Li, J. Enabling aqueous processing for LiNi0.80Co0.15Al0.05O2 (NCA)-based lithium-ion battery cathodes using polyacrylic acid. *Electrochim. Acta* **2021**, *380*, 138203. [CrossRef]

38. Versaci, D.; Apostu, O.D.; Dessantis, D.; Amici, J.; Francia, C.; Minella, M.; Bodoardo, S. Tragacanth, an Exudate Gum as Suitable Aqueous Binder for High Voltage Cathode Material. *Batteries* **2023**, *9*, 199. [CrossRef]

39. Li, J.; Lewis, R.B.; Dahn, J.R. Sodium Carboxymethyl Cellulose. *Electrochem. Solid-State Lett.* **2007**, *10*, A17–A20. [CrossRef]

40. Hu, H.; Tao, B.; He, Y.; Zhou, S. Effect of Conductive Carbon Black on Mechanical Properties of Aqueous Polymer Binders for Secondary Battery Electrode. *Polymers* **2019**, *11*, 1500. [CrossRef]

41. Koo, B.; Kim, H.; Cho, Y.; Lee, K.T.; Choi, N.; Cho, J. A Highly Cross-Linked Polymeric Binder for High-Performance Silicon Negative Electrodes in Lithium Ion Batteries. *Angew. Chem. Int. Ed.* **2012**, *51*, 8762–8767. [CrossRef]

42. Myung, S.-T.; Hitoshi, Y.; Sun, Y.-K. Electrochemical behavior and passivation of current collectors in lithium-ion batteries. *J. Mater. Chem.* **2011**, *21*, 9891–9911. [CrossRef]

43. Surace, Y.; Jeschull, F.; Schott, T.; Zürcher, S.; Spahr, M.E.; Trabesinger, S. Improving the Cycling Stability of SnO_2–Graphite Electrodes. *ACS Appl. Energy Mater.* **2019**, *2*, 7364–7374. [CrossRef]

44. Surace, Y.; Jeschull, F.; Novák, P.; Trabesinger, S. Performance-Determining Factors for Si–Graphite Electrode Evaluation: The Role of Mass Loading and Amount of Electrolyte Additive. *J. Electrochem. Soc.* **2023**, *170*, 020510. [CrossRef]

45. Bigoni, F.; De Giorgio, F.; Soavi, F.; Arbizzani, C. Sodium Alginate: A Water-Processable Binder in High-Voltage Cathode Formulations. *J. Electrochem. Soc.* **2017**, *164*, A6171–A6177. [CrossRef]

46. Bizot, C.; Blin, M.-A.; Guichard, P.; Soudan, P.; Gaubicher, J.; Poizot, P. Aluminum current collector for high voltage Li-ion battery. Part II: Benefit of the En' Safe® primed current collector technology. *Electrochem. Commun.* **2021**, *126*, 107008. [CrossRef]